

Research Article

Synchronization of Complex Dynamical Networks with Hybrid Time Delay under Event-Triggered Control: The Threshold Function Method

Fei Wang ¹, Zhaowen Zheng ¹, and Yongqing Yang²

¹School of Mathematical Sciences, Qufu Normal University, Qufu 273165, Shandong, China

²School of Science, Jiangnan University, Wuxi 214122, Jiangsu, China

Correspondence should be addressed to Fei Wang; fei_9206@163.com

Received 15 July 2019; Revised 26 October 2019; Accepted 14 November 2019; Published 7 December 2019

Academic Editor: Eric Campos-Canton

Copyright © 2019 Fei Wang et al. This is an open access article distributed under the Creative Commons Attribution License, which permits unrestricted use, distribution, and reproduction in any medium, provided the original work is properly cited.

This paper investigates the synchronization of general complex dynamical networks (CDNs) with both internal delay and transmission delay. Event-triggered mechanism is applied for the feedback controllers, in which the triggered function is formed as a nonincreasing function. Both continuous feedback and sampled-data feedback methods are studied. According to Lyapunov stability theorem and generalized Halanay's inequality, quasi-synchronization criteria are derived at first. The synchronization error is bounded with some parameters of the triggered function. Then, the completed synchronization can be guaranteed as a special case. Finally, coupled neural networks as numerical simulation examples are given to verify the theoretical results.

1. Introduction

In the last few decades, models formed as coupled networks have been applied to many fields, such as biology neural networks, ecological networks, Internet, WWW (World Wide Web), and so on [1–3]. Consequently, the CDNs (complex dynamical networks) have attracted much attention from a large number of researchers. There were also some topics in the investigations of CDNs. Among which, synchronization behaviors is one of the most important topics due to its applications in communication system, consensus, distributed computing, formation control and image processing, and so on [4–6]. Many results about synchronization of CDNs have been published in recent years, which could be seen in [7–14] and referenced there in.

However, there are some networks that cannot be synchronized by their own internal structure; thus, some controllers have been designed to force them to synchronize. Some works have investigated the synchronization of the complex dynamical networks via control strategies in recent years [15–18]. For example, in [19], the problem of

synchronization control of complex dynamical networks subject to nonlinear couplings and uncertainties has been investigated. In [20], the pinning impulsive synchronization problem for a class of complex dynamical networks with time-varying delay has been summarized. The exponential synchronization of Lur'e type complex dynamical networks with uncertain coupling strength has been studied in [21]. Synchronization of CDNs under actuator saturation has been investigated in [9, 22]. In the above results, signals were transferred real-time among networks. However, it may not fit for the real world systems. With the fast development of digital signal technologies, the sampled-data control has catered to people by its lower cost than continuous control approaches. Some results about synchronization of CDNs with sampled-data controllers were existed. The first result about the sampled-data synchronization control of CDNs was investigated in [23]. In [24], the stochastic sampled-data control method has been applied to the synchronization of CDNs. The synchronization problem for a class of complex delayed dynamical networks by using the sampled-data feedback control has been studied in [25], in which, reciprocally convex technique and a novel class of integral

inequalities have also been used. The sampled-data synchronization problem of chaotic Lur'e systems by using sampled output of the systems with variable sampling rates has been studied in [26], and so on.

Results in the aforementioned sampled-data feedback control, data of controllers often update continuous or period. Note that the signals of controllers were updated at a fixed rate regardless, whether they are really necessary or not. Naturally, there must be some unnecessary updates in the sampled-data control strategy. Recently, a new effective strategy has been presented, which was named as event-triggered control or event-driven control. Under the event-triggered mechanism, controllers will be updated as well as the occurrence of a designed event. It is obviously that the energy can be saved compared with the continuous updating or period updating. The analysis of the feedback control system with event-triggered scheme has drawn much attention in the last few years. For example, event-triggered sliding mode control for uncertain stochastic systems has been studied in [27]. In [28], the leader-following consensus for multiagent systems with general linear dynamics by means of event-triggered scheme has been investigated. The networked synchronization communication for nonlinear uncertain fractional-order chaotic systems via the event-triggered control method was investigated in [29]. Two survey papers survey recent advances in event-triggered communication and control has been published recently [30, 31]. There were also a number of works concerning the event-triggered control for the synchronization control problem, which can be found in [32–39] and references there in.

According to the above existing works on the event-triggered consensus of multiagent systems, one can conclude that the event-triggered conditions are designed to estimate the change of system's errors, which means that when errors converge to zeros, the event would not be triggered. It is a natural idea to design an event with a threshold about system's errors. In [40], a constant event threshold has been designed, when measure errors are larger than the threshold, the event would be triggered. After that, a new exponentially decreasing event threshold condition has been proposed in [41]. Compared to some other designed events in above results, this kind of event condition is easier to analyse stability due to some fine properties of the exponential function.

This paper investigates the synchronization problem for complex dynamical networks; both continuous feedback control and sampled-data feedback control will be studied. Inspired by the results of [41, 42], a nonincreasing event threshold function is used as the condition to define an event, quasi-synchronization can be reached. The trajectory of the error system exponentially converges to the bounded region which is related to the parameters of the threshold function. Furthermore, complete synchronization can be guaranteed with appropriate parameters in the threshold function.

Indeed, our recent work has been published in [43], which has considered a simple CDN model without time delay. However, time delays cannot be unavoidable in real-

world systems, which also could lead to some complex dynamical behaviors such as chaos. In the CDNs, the time delays also exist when information is transferring among nodes. Consequently, this paper will consider the internal delays of each node and transmission delays among nodes. The main contribution of this paper could be concluded as follows: first, a general CDN model with hybrid time delay has been considered in this paper, the model in [43] was a special case of this paper. Second, the synchronization can be reached under the event-triggered control method, in which, a kind of monotone nonincreasing threshold function is applied for the triggered function. Third, both continuous feedback and sampled-data feedback method are studied, and the Zeno behavior has been excluded in the continuous case.

The rest of the paper is organized as follows: in Section 2, we introduce some definitions and some lemmas which are necessary for presenting our results in the following. The main results about the synchronization control problem are presented in Section 3. Then, some examples are given to demonstrate the effectiveness of our results in Section 4. Conclusions are finally drawn in Section 5.

Notations. Let \mathbb{R} be the set of real numbers. \mathbb{R}^n and $\mathbb{R}^{n_1 \times n_2}$ refer to the n -dimensional real vector and $n_1 \times n_2$ real matrices. The superscript “ T ” denotes matrix transposition. I_n denotes the n -dimensional identity matrix. For a vector $x \in \mathbb{R}^n$, x is defined as $\|x\| = \sqrt{x^T x}$. For $P \in \mathbb{R}^{n \times n}$, $\lambda_{\max}(P)$ represents the maximum eigenvalue of P . \otimes denotes Kronecker product. $C([- \tau, 0], \mathbb{R}^n)$ denotes the set of all n -dimensional continuous functions defined on the interval $[- \tau, 0]$.

2. Preliminaries

Consider a complex dynamical network with N nodes, and the dynamics of the i^{th} node is described by

$$\begin{aligned} \dot{x}_i(t) = & f(t, x_i(t), x_i(t - \tau_1(t))) + c_1 \sum_{j=1}^N a_{ij} \Gamma_1 (x_j(t) - x_i(t)) \\ & + c_2 \sum_{j=1}^N b_{ij} \Gamma_2 (x_j(t - \tau_2(t)) - x_i(t - \tau_2(t))) + u_i(t), \end{aligned} \quad (1)$$

where $x_i(t) = (x_{i1}(t), x_{i2}(t), \dots, x_{in}(t))^T \in \mathbb{R}^n$ ($i = 1, 2, \dots, N$) is the state variables of the i^{th} node. $f: \mathbb{R} \times \mathbb{R}^n \times \mathbb{R}^n \rightarrow \mathbb{R}^n$ is a continuously vector value function. $\tau_1(t) \in [0, \tau_1]$ represents the internal delay occurring inside the node; $\tau_2(t) \in [0, \tau_2]$ denotes the transmission delay for the signal sent from j^{th} node to i^{th} node, where τ_1, τ_2 are known constants. $u_i(t)$ is the control input which will be given later. $\Gamma_1, \Gamma_2 \in \mathbb{R}^{n \times n}$ are diagonal matrices with positive diagonal elements. $A = (a_{ij}) \in \mathbb{R}^{N \times N}$ and $B = (b_{ij}) \in \mathbb{R}^{N \times N}$ are the weight configuration matrices. If there is a connection from node i to node j , then $a_{ij} = a_{ji} > 0$, $b_{ij} = b_{ji} > 0$; otherwise, $a_{ij} = a_{ji} = b_{ij} = b_{ji} = 0$. The diagonal elements of matrix A and B are defined by

$$a_{ii} = - \sum_{j=1, j \neq i}^N a_{ij}, \quad (2)$$

$$b_{ii} = - \sum_{j=1, j \neq i}^N b_{ij}.$$

The initial values associated with system (1) are $x_i(t) = \phi_i(t) \in \mathbb{C}([- \tau, 0]; \mathbb{R}^n)$ ($i = 1, 2, \dots, N$), where $\tau = \max\{\tau_1, \tau_2\}$. Let $s(t)$ be a solution of the isolated dynamic system:

$$\dot{s}(t) = f(t, s(t), s(t - \tau_1(t))). \quad (3)$$

The initial values of the isolated dynamic system is defined as $s(t) = \phi^s(t) \in \mathbb{C}([- \tau, 0]; \mathbb{R}^n)$. Here, $s(t)$ may be an equilibrium point, a periodic orbit, or even a chaotic orbit. In this paper, the objective trajectory that the non-linear dynamical network (1) will be forced to $s(t)$.

Let $e_i(t) = x_i(t) - s(t)$, for $i = 1, 2, \dots, N$. According to (2), one has

$$\sum_{j=1}^N a_{ij} \Gamma_1 s(t) = \sum_{j=1}^N b_{ij} \Gamma_2 s(t - \tau_2(t)) = 0, \quad (4)$$

$$\sum_{j=1}^N b_{ij} \Gamma_2 x_j(t - \tau_2(t)) = 0.$$

Then,

$$\begin{aligned} \dot{e}_i(t) &= \dot{x}_i(t) - \dot{s}(t) \\ &= \tilde{f}(t, e_i(t), e_i(t - \tau_1(t))) + c_1 \sum_{j=1}^N a_{ij} \Gamma_1 (x_j(t) - s(t) \\ &\quad - (x_i(t) - s(t))) + c_2 \sum_{j=1}^N b_{ij} \Gamma_2 (x_j(t - \tau_2(t)) \\ &\quad - x_i(t - \tau_3(t))) + c_2 \sum_{j=1}^N b_{ij} \Gamma_1 (s(t - \tau_2(t)) \\ &\quad - s(t - \tau_2(t))) + u_i(t) \\ &= \tilde{f}(t, e_i(t), e_i(t - \tau_1(t))) + c_1 \sum_{j=1}^N a_{ij} \Gamma_1 (e_j(t) - e_i(t)) \\ &\quad + c_2 \sum_{j=1}^N b_{ij} \Gamma_2 (e_j(t - \tau_2(t)) - e_i(t - \tau_2(t))) + u_i(t), \end{aligned} \quad (5)$$

where $\tilde{f}(t, e_i(t), e_i(t - \tau_1(t))) = f(t, x_i(t), x_i(t - \tau_1(t))) - f(t, s(t), s(t - \tau_1(t)))$. Then, the error dynamics could be described by

$$\begin{aligned} \dot{e}_i(t) &= \tilde{f}(t, e_i(t), e_i(t - \tau_1(t))) + c_1 \sum_{j=1}^N a_{ij} \Gamma_1 e_j(t) \\ &\quad + c_2 \sum_{j=1}^N b_{ij} \Gamma_2 e_j(t - \tau_2(t)) + u_i(t). \end{aligned} \quad (6)$$

The initial conditions associated with the error systems are $e_i(t) = \psi_i(t) = \phi_i(t) - \phi^s(t) \in \mathbb{C}([- \tau, 0]; \mathbb{R}^n)$. It is easy to see that the globally exponential synchronization of the

controlled delayed dynamical network (1) is achieved if the zero solution of the error dynamical system is globally exponentially stable. To proceed with the following definition, assumptions and lemmas are given.

Definition 1 (see [13]). The dynamic network (1) is said to achieve quasi-synchronization with an error bound $\epsilon > 0$, if there exists a compact set Ω such that, for any $\phi_i(t), \phi^s(t) \in \mathbb{C}([- \tau, 0]; \mathbb{R}^n)$, the error signal $e_i(t) = x_i(t) - s(t)$ converges into the set $\Omega = \{e(t) \mid \|e(t)\| \leq \epsilon\}$ as $t \rightarrow +\infty$.

Assumption 1 (see [20]). For the vector-valued function $f(t, x(t), x(t - \tau_1(t)))$, suppose for any $x(t) \in \mathbb{R}^n$, $y(t) \in \mathbb{R}^n$, there exists positive constants $L_1 > 0$ and $L_2 > 0$ such that

$$\begin{aligned} (x(t) - y(t))^T (f(t, x(t), x(t - \tau_1(t))) - f(t, y(t), y(t - \tau_1(t)))) \\ \leq L_1 \|x(t) - y(t)\|^2 + L_2 \|(x(t - \tau_1(t)) - y(t - \tau_1(t)))\|^2. \end{aligned} \quad (7)$$

Assumption 2 (see [44]). For the vector-valued function $f(t, x(t), x(t - \tau_1(t)))$, suppose for any $x(t) \in \mathbb{R}^n$, $y(t) \in \mathbb{R}^n$, there exists positive constants $L_{f1} > 0$ and $L_{f2} > 0$ such that

$$\begin{aligned} \|(f(t, x(t), x(t - \tau_1(t))) - f(t, y(t), y(t - \tau_1(t))))\| \\ \leq L_{f1} \|x(t) - y(t)\| + L_{f2} \|(x(t - \tau_1(t)) - y(t - \tau_1(t)))\|. \end{aligned} \quad (8)$$

Lemma 1 (see [45]). For matrices A, B, C , and D with appropriate dimensions, the Kronecker product \otimes satisfies

$$\begin{aligned} (A + B) \otimes C &= A \otimes C + B \otimes C; \\ (A \otimes B)(C \otimes D) &= (AC) \otimes (BD); \\ (A^T \otimes B^T) &= (A \otimes B)^T; \\ \lambda_{\max}(A \otimes B) &= \lambda_{\max}(A) \lambda_{\max}(B). \end{aligned} \quad (9)$$

Lemma 2 (generalized Halanay's inequality) (see [46]). If $u(t) \geq 0$, $t \in (-\infty + \infty)$, and

$$\begin{aligned} \dot{u}(t) &\leq \gamma(t) + \alpha(t)u(t) + \beta(t) \sup_{t - \tau(t) \leq \xi \leq t} u(\xi) (t \geq t_0), u(t) \\ &= |\Psi(t)| (t \leq t_0), \end{aligned} \quad (10)$$

where $\Psi(t)$ is bounded and continuous for $t \leq t_0$, continuous functions $\gamma(t) \geq 0$, $\beta(t) \geq 0$, and $\alpha(t) \leq 0$ for $t \in [t_0, +\infty)$, $\tau(t) \geq 0$, and if there exists $\sigma > 0$ such that

$$\alpha(t) + \beta(t) \leq -\sigma < 0 \text{ for } t \geq t_0, \quad (11)$$

then we have

$$u(t) \leq \frac{\gamma^*}{\sigma} + Ge^{-\mu^*(t-t_0)}, \quad t \geq t_0, \quad (12)$$

where G , γ^* , and μ^* are defined as the following: $G = \sup_{-\infty < \xi \leq t_0} |\Psi(t)|$, $\gamma^* = \sup_{t_0 \leq t < +\infty} \gamma(t)$, and $\mu^* = \inf_{t \geq t_0} \{\mu(t) : \mu(t) + \alpha(t) + \beta(t)e^{\mu(t)\tau(t)} = 0\}$.

3. Main Results

In this paper, both continuous feedback controllers and sampled-data feedback controllers are adopted; meanwhile, the controller considered in this paper is event-triggered.

3.1. Event-Triggered Control Method Based on Continuous Feedback. A continuous feedback controller is defined as

$$u_i(t) = -d_i(x_i(t) - s(t)). \quad (13)$$

When we consider the event-triggered strategy, controllers will be updated when an event has been triggered instead of in a continuous time. More specifically, let us denote the time instants for i^{th} node when an event happens by $\{t_0^i, t_1^i, \dots\}$ with $t_k^i < t_{k+1}^i$. The controller for i^{th} can be described as

$$u_i(t) = -d_i(x_i(t_k^i) - s(t_k^i)), \quad t \in [t_k^i, t_{k+1}^i), \quad (14)$$

where d_i is the feedback gain to be determined. Without loss generality, the first event is generated at time t_0 for all nodes. For i^{th} node, the event-triggering time instants are defined as follows:

$$t_{k+1}^i = \inf\{t > t_k^i \mid \|\delta_i(t)\| \geq \theta(t)\}, \quad (15)$$

where $\delta_i(t) = e_i(t_k^i) - e_i(t)$ and $\theta(t) = \sqrt{\theta_0 + \alpha\varepsilon^{-\beta t}}$ is the exponentially decreasing event threshold with given parameters $\varepsilon > 1$, $\beta \geq 0$, $\alpha > 0$, and $\theta_0 \geq 0$. Under controller (14), the synchronization error system can be rewritten as

$$\begin{aligned} \dot{e}_i(t) = & \tilde{f}(t, e_i(t), e_i(t - \tau_1(t))) + c_1 \sum_{j=1}^N a_{ij} \Gamma_1 e_j(t) \\ & + c_2 \sum_{j=1}^N b_{ij} \Gamma_2 e_j(t - \tau_2(t)) - d_i e_i(t_k^i), \quad t \in [t_k^i, t_{k+1}^i). \end{aligned} \quad (16)$$

Theorem 1. Suppose that Assumption 1 holds. If there exist positive constants p , q , ω_1 , ω_2 , and d_i such that

- (1) $(a + L_1 + p)I_N - (2 - \omega_2)D < 0$,
- (2) $p - q > 0$,

where $a = 2c_1 \lambda_{\max}(A \otimes \Gamma_1) + c_2 \omega_1 \lambda_{\max}((BB^T) \otimes (\Gamma_2 \Gamma_2^T))$, $D = \text{diag}(d_1, d_2, \dots, d_N)$, and $q = L_2 + (c_2/\omega_1)$. Then, the controlled delayed dynamical network (1) can achieve quasi-synchronization, and the trajectory of the error system exponentially converges to the bounded region $\Omega(\theta_0) = \{e(t) \mid \|e(t)\| \leq \sqrt{d^* N \theta_0 / \omega_2 (p - q)}\}$, where $d^* = \max\{d_1, d_2, \dots, d_N\}$.

Proof. Considering the following Lyapunov function

$$V(t) = \|e(t)\|^2 = \sum_{i=1}^N \|e_i(t)\|^2 = e^T(t)e(t) = \sum_{i=1}^N e_i^T(t)e_i(t), \quad (17)$$

calculating the derivatives of $V(t)$ along the solutions of system (16), one has

$$\begin{aligned} \dot{V}(t) = & 2 \sum_{i=1}^N e_i^T(t) \dot{e}_i(t) \\ = & 2 \sum_{i=1}^N e_i^T \left(\tilde{f}(t, e_i(t), e_i(t - \tau_1(t))) + c_1 \sum_{j=1}^N a_{ij} \Gamma_1 e_j(t) \right. \\ & \left. + c_2 \sum_{j=1}^N b_{ij} \Gamma_2 e_j(t - \tau_2(t)) - d_i e_i(t_k^i) \right) \\ = & 2 \sum_{i=1}^N e_i^T(t) \tilde{f}(t, e_i(t), e_i(t - \tau_1(t))) \\ & + 2c_1 \sum_{i=1}^N e_i^T(t) \sum_{j=1}^N a_{ij} \Gamma_1 e_j(t) + 2c_2 \sum_{i=1}^N e_i^T(t) \sum_{j=1}^N b_{ij} \Gamma_2 e_j \\ & \cdot (t - \tau_2(t)) - 2 \sum_{i=1}^N d_i e_i^T(t) e_i(t_k^i). \end{aligned} \quad (18)$$

Based on Assumption 1, we have

$$\begin{aligned} 2 \sum_{i=1}^N e_i^T(t) \tilde{f}(t, e_i(t), e_i(t - \tau_1(t))) & \leq L_1 \sum_{i=1}^N \|e_i(t)\|^2 \\ & + L_2 \sum_{i=1}^N \|e_i(t - \tau_1(t))\|^2 \\ = & L_1 e^T(t)e(t) + L_2 e^T \\ & \cdot (t - \tau_1(t))e(t - \tau_1(t)). \end{aligned} \quad (19)$$

By using the Kronecker product of the matrices, the second term and the third term can be written in the following compact matrix form:

$$\begin{aligned} 2c_1 \sum_{i=1}^N e_i^T(t) \sum_{j=1}^N a_{ij} \Gamma_1 e_j(t) & = 2c_1 e(t)^T (A \otimes \Gamma_1) e(t), \\ 2c_2 \sum_{i=1}^N e_i^T(t) \sum_{j=1}^N b_{ij} \Gamma_2 e_j(t - \tau_2(t)) & = 2c_2 e(t)^T (B \otimes \Gamma_2) e \\ & \cdot (t - \tau_2(t)). \end{aligned} \quad (20)$$

According to $x^T y = y^T x = (1/2)(x^T y + y^T x) \leq (\varepsilon/2)x^T x + (1/2\varepsilon)y^T y$, the following inequalities can be derived:

$$\begin{aligned}
2c_2e(t)^T(B\otimes\Gamma_2)e(t-\tau_2(t)) &\leq c_2\omega_1e^T(t)((B\otimes\Gamma_2)(B\otimes\Gamma_2)^T)e \\
&\quad \cdot (t) + \frac{c_2}{\omega_1}e^T(t-\tau_2(t))e(t-\tau_2(t)) \\
&= c_2\omega_1e^T(t)((BB^T)\otimes(\Gamma_2\Gamma_2^T))e \\
&\quad \cdot (t) + \frac{c_2}{\omega_1}e^T(t-\tau_2(t)) \\
&\quad \cdot (I_N\otimes I_n)e(t-\tau_2(t)).
\end{aligned} \tag{21}$$

The last term will be handled as follows:

$$\begin{aligned}
-2\sum_{i=1}^Nd_i e_i^T(t)e_i(t_k^i) &= -2\sum_{i=1}^Nd_i e_i^T(t)(e_i(t)+\delta_i(t)) \\
&= -2\sum_{i=1}^Nd_i e_i^T(t)e_i(t) - 2\sum_{i=1}^Nd_i(e_i^T(t)\delta_i(t)) \\
&\leq -2e^T(t)(D\otimes I_n)e(t) + \sum_{i=1}^Nd_i \\
&\quad \cdot \left(\omega_2e_i^T(t)e_i(t) + \frac{1}{\omega_2}\delta_i^T(t)\delta_i(t)\right) \\
&= -(2-\omega_2)e^T(t)(D\otimes I_n)e(t) \\
&\quad + \frac{1}{\omega_2}\sum_{i=1}^Nd_i\|\delta_i(t)\|^2 \\
&\leq -(2-\omega_2)e^T(t)(D\otimes I_n)e(t) + \frac{d^*N}{\omega_2}\alpha\varepsilon^{-\beta t} \\
&\quad + \frac{d^*N\theta_0}{\omega_2}.
\end{aligned} \tag{22}$$

Then, one can derive

$$\begin{aligned}
\dot{V}(t) &\leq L_1e^T(t)(I_N\otimes I_n)e(t) + L_2e^T(t-\tau_1(t))(I_N\otimes I_n)e \\
&\quad \cdot (t-\tau_1(t)) + 2c_1e(t)^T(A\otimes\Gamma_1)e(t) \\
&\quad + c_2\omega_1e^T(t)((BB^T)\otimes(\Gamma_2\Gamma_2^T))e(t) + \frac{c_2}{\omega_1}e^T(t-\tau_2(t)) \\
&\quad \cdot (I_N\otimes I_n)e(t-\tau_2(t)) - (2-\omega_2)e^T(t)(D\otimes I_n)e(t) \\
&\quad + \frac{d^*N}{\omega_2}\alpha\varepsilon^{-\beta t} + \frac{d^*N\theta_0}{\omega_2} \\
&= e^T(t)(L_1(I_N\otimes I_n) + 2c_1(A\otimes\Gamma_1) + c_2\omega_1((BB^T)\otimes(\Gamma_2\Gamma_2^T)) \\
&\quad - (2-\omega_2)(D\otimes I_n))e(t) \\
&\quad + e^T(t-\tau_2(t))\left(L_2(I_N\otimes I_n) + \frac{c_2}{\omega_1}(I_N\otimes I_n)\right) \\
&\quad \cdot e(t-\tau_2(t)) + \frac{d^*N}{\omega_2}\alpha\varepsilon^{-\beta t} + \frac{d^*N\theta_0}{\omega_2} \\
&\leq -pV(t) + q\sup_{t-\tau\leq s\leq t}V(s) + \gamma(t),
\end{aligned} \tag{23}$$

where $\gamma(t) = (d^*N/\omega_2)\alpha\varepsilon^{-\beta t} + (d^*N\theta_0/\omega_2)$; it is easy to get $\gamma^* = \sup_{t_0\leq t<+\infty}\gamma(t) = (d^*N\theta_0/\omega_2)$. By Lemma 2 and condition (2) of Theorem 1, the following result can be obtained:

$$V(t) \leq \frac{\gamma^*}{p-q} + \Psi e^{-\mu^*(t-t_0)}, \quad t \geq t_0, \tag{24}$$

where $\Psi = \sup_{-\tau\leq s\leq t_0}V(s)$ and μ^* is a root of the equation $\mu - p + qe^{\tau\mu} = 0$. It is obvious that $\mu^* > 0$; then, we can conclude that the error system converges exponentially to the set $\Omega(\theta_0) = \{e(t) \mid \|e(t)\| \leq \sqrt{d^*N\theta_0/\omega_2(p-q)}\}$ can be guaranteed, and according to Definition 1, the controlled delayed dynamical network (1) can achieve quasi-synchronization. The proof is thus completed.

In order to exclude Zeno behavior, the following theorem shows that the interevent times are lower-bounded by a positive constant in the following theorem. \square

Theorem 2. *Suppose that Assumption 2 and all conditions of Theorem 1 hold. With the triggered instants determined by (15), the Zeno behavior can be excluded for all plants in the network, which means that the minimum interevent interval for all plants is lower-bounded by a positive scalar.*

Proof. To prove this theorem, $\|\dot{e}_i(t)\|$ is bounded which will be derived at first, and then the Zeno behavior will be excluded.

By using the triangular inequality, it is easy to get

$$\begin{aligned}
\|\dot{e}_i(t)\| &= \left\| \tilde{f}(t, e_i(t), e_i(t-\tau_1(t))) + c_1\sum_{j=1}^Na_{ij}\Gamma_1e_j(t) \right. \\
&\quad \left. + c_2\sum_{j=1}^Nb_{ij}\Gamma_2e_j(t-\tau_2(t)) - d_i e_i(t_k^i) \right\| \\
&\leq \|f(t, x_i(t), x_i(t-\tau_1(t))) - f(t, s(t), s(t-\tau_1(t)))\| \\
&\quad + c_1\sum_{j=1}^Na_{ij}\gamma_1\|e_j(t)\| + c_2\sum_{j=1}^Nb_{ij}\gamma_2\|e_j(t-\tau_2(t))\| \\
&\quad + d_i(\|e_i(t)\| + \|\delta_i(t)\|) \\
&\leq (L_{f_1} + d_i)\|e_i(t)\| + L_{f_2}\|e_i(t-\tau_1(t))\| \\
&\quad + c_1\sum_{j=1}^Na_{ij}\gamma_1\|e_j(t)\| + c_2\sum_{j=1}^Nb_{ij}\gamma_2\|e_j(t-\tau_2(t))\| \\
&\quad + d_i\|\delta_i(t)\|,
\end{aligned} \tag{25}$$

where $\gamma_1 = \|\Gamma_1\|$ and $\gamma_2 = \|\Gamma_2\|$. According to the results in Theorem 1, we have

$$\|e_i(t)\| \leq \|e(t)\| \leq \sqrt{V(t)} \leq \sqrt{\frac{\gamma^*}{p-q}} + \Psi, \quad t \in [-\tau, +\infty), \tag{26}$$

where p, q, γ^* , and Ψ have been defined in Theorem 1. Then,

$$\begin{aligned} \|\dot{e}_i(t)\| &\leq (L_{f_1} + L_{f_2} + d_i - 2c_1\gamma_1 a_{ii} - 2c_2\gamma_2 b_{ii}) \\ &\quad \cdot \sqrt{\frac{\gamma^*}{p-q}} + \Psi + d_i \|\delta_i(t)\| \\ &\leq M + d_i \theta(t), \end{aligned} \quad (27)$$

where $M = (L_{f_1} + L_{f_2} + d_i - 2c_1\gamma_1 a_{ii} - 2c_2\gamma_2 b_{ii}) \sqrt{\gamma^*/(p-q)} + \Psi$ is a bounded constant. For $t \in [t_k^i, t_{k+1}^i)$, noting that $\delta_i(t) = \int_{t_k^i}^t \delta_i(s) ds = - \int_{t_k^i}^t \dot{e}_i(s) ds$, one has

$$\begin{aligned} \|\delta_i(t)\| &= \left\| \int_{t_k^i}^t \dot{e}_i(s) ds \right\| \leq \int_{t_k^i}^t \|\dot{e}_i(s)\| ds \\ &\leq M(t - t_k^i) + d_i \int_{t_k^i}^t \theta(s) ds \\ &\leq (M + (\theta_0 + \alpha)d_i)(t - t_k^i). \end{aligned} \quad (28)$$

According to the triggered instants determined by (15), the next event will not be generated before $\|\delta_i(t^*)\| = \theta(t^*)$; denote $T = t^* - t_k^i$, then,

$$\sqrt{\theta_0 + \alpha \varepsilon^{-\beta(T+t_k^i)}} \leq (M + (\theta_0 + \alpha)d_i)T. \quad (29)$$

Let $q(T) = \sqrt{\theta_0 + \alpha \varepsilon^{-\beta(T+t_k^i)}} - (M + (\theta_0 + \alpha)d_i)T$, one has $q(0) > 0$, and when $T \rightarrow +\infty$, $q(T) < 0$; furthermore, $q(T)$ is monotonically decreasing. Thus, to obtain the above inequality, there must be $T \geq T^* > 0$. It can be concluded that there exists a positive lower bound of the minimum interevent interval. This completes the proof. \square

Remark 1. Note that ε , β , and α in the threshold function $\theta(t)$ cannot affect the region of synchronization error. However, from (29), one can find that those parameters may affect the lower bound of the minimum interevent interval. The parameter M has included a_{ii} and b_{ii} , which are determined by the topology of networks.

Remark 2. θ_0 is not a parameter of controllers, and it can be adjusted free. According to the result in Theorem 1, the

$$\begin{aligned} e(t - \hat{\tau}(t)) &= (e_1(t - \hat{\tau}_1(t)), e_2(t - \hat{\tau}_2(t)), \dots, e_N(t - \hat{\tau}_N(t)))^T, \\ e(t - \tau_2(t)) &= (e_1(t - \tau_2(t)), e_2(t - \tau_2(t)), \dots, e_N(t - \tau_2(t))), \\ \bar{F}(t, e(t), e(t - \tau_1(t))) &= (\bar{f}(t, e_1(t), e_1(t - \tau_1(t))), \bar{f}(t, e_2(t), e_2(t - \tau_1(t))), \dots, \bar{f}(t, e_N(t), e_N(t - \tau_1(t))))^T, \\ \dot{e}(t) &= (\dot{e}_1(t), \dot{e}_2(t), \dots, \dot{e}_N(t))^T. \end{aligned} \quad (34)$$

Theorem 3. *The controlled delayed dynamical network (1) can achieve quasi-synchronization under controller (31), and the trajectory of the error system exponentially*

synchronization error will be bounded by a parameter related with θ_0 . In addition, the complete synchronization can be guaranteed when $\theta_0 = 0$, which will be checked in the simulation part. Furthermore, when $\theta_0 = 0$, the Zeno behavior still can be excluded.

3.2. Event-Triggered Control Method Based on Sampled-Data Feedback. A sampled-data feedback controller is defined as

$$u_i(t) = -d_i(x_i(mT) - s(mT)), \quad (30)$$

where T is the sampling period, $m = 0, 1, \dots$. Under the event-triggered strategy, the data will be updated when the designed event was triggered, instead of in every sampled time. The controller for i^{th} can be described as

$$u_i(t) = -d_i(x_i(t_k^i) - s(t_k^i)), \quad t \in [t_k^i, t_{k+1}^i), \quad (31)$$

where $t_k^i = h_k^i T$ means that k^{th} trigger for i^{th} node at h_k^i sample, $h_k^i = 0, 1, \dots$ and $h_0^i = 0$. For i^{th} node, the event-triggering time instants are defined as follows:

$$h_{k+1}^i = \min_{j \in \mathbb{Z}} \{j > h_k^i \mid \|\delta_i(jT)\| \geq \theta((j+1)T)\}, \quad (32)$$

where $\delta_i^s((h_k^i + j)T) = e_i(t_k^i) - e_i((h_k^i + j)T)$, $j = 1, 2, \dots$. Let us define $\hat{\tau}_i(t) = t - (h_k^i + j)T$ for i^{th} node during $t \in [(h_k^i + j)T, (h_k^i + j + 1)T)$. Under controller (14), the synchronization error system can be rewritten as

$$\begin{aligned} \dot{e}_i(t) &= \tilde{f}(t, e_i(t), e_i(t - \tau_1(t))) + c_1 \sum_{j=1}^N a_{ij} \Gamma_1 e_j(t) \\ &\quad + c_2 \sum_{j=1}^N b_{ij} \Gamma_2 e_j(t - \tau_2(t)) - d_i(e_i(t - \hat{\tau}_i(t)) \\ &\quad + \delta_i^s(t - \hat{\tau}_i(t))). \end{aligned} \quad (33)$$

The following vector symbols will be used later:

converges to the bounded region $\Omega(\theta_0) = \{e(t) \mid \|e(t)\| \leq \sqrt{N\theta_0/2\xi}\}$ if there exist matrices $P > 0$, $Q > 0$, $R > 0$, and $S > 0$ such that

$$\Xi_0 = \begin{pmatrix} \Xi_{11} & \Xi_{12} & \Xi_{13} & \Xi_{14} & \Xi_{15} \\ * & 0 & 0 & 0 & \Xi_{25} \\ * & * & 0 & 0 & \Xi_{35} \\ * & * & * & 0 & \Xi_{45} \\ * & * & * & * & \Xi_{55}^0 \end{pmatrix} < 0, \quad (35)$$

$$\Xi_T = \begin{pmatrix} \Xi_{11} & \Xi_{12} & \Xi_{13} & \Xi_{14} & \Xi_{15} & 0 \\ * & 0 & 0 & 0 & \Xi_{25} & 0 \\ * & * & 0 & 0 & \Xi_{35} & 0 \\ * & * & * & 0 & \Xi_{45} & 0 \\ * & * & * & * & \Xi_{55}^{(T)} & 0 \\ * & * & * & * & * & \Xi_{66}^{(T)} \end{pmatrix} < 0, \quad (36)$$

where $\xi > 0$ is a given decay rate,

$$\begin{aligned} \Xi_{11} &= 2\xi(I_N \otimes P) + 2c_1(A \otimes R\Gamma_1) + DD^T \otimes RR^T, \\ \Xi_{12} &= c_2(B \otimes R\Gamma_2), \\ \Xi_{13} &= -(D \otimes R), \\ \Xi_{14} &= (I_N \otimes R), \\ \Xi_{15} &= -(I_N \otimes R) + c_1(A \otimes S\Gamma_1)^T + \frac{(I_N \otimes P)}{2}, \\ \Xi_{25} &= c_2(B \otimes S\Gamma_2)^T, \\ \Xi_{35} &= -(D \otimes S), \\ \Xi_{45} &= (I_N \otimes S), \\ \Xi_{55}^{(0)} &= T(I_N \otimes Q) - 2(I_N \otimes S) + (DD^T \otimes SS^T), \\ \Xi_{55}^{(T)} &= -2(I_N \otimes S) + (DD^T \otimes SS^T), \\ \Xi_{66}^{(T)} &= Te^{-2\xi T}(I_N \otimes Q). \end{aligned} \quad (37)$$

Proof. Considering the following Lyapunov function

$$V(t) = \sum_{i=1}^N e_i^T P e_i(t) + \sum_{i=1}^N (T - \hat{\tau}_i(t)) \int_{t-\hat{\tau}_i(t)}^t e^{2\xi(s-t)} \dot{e}_i^T(s) Q \dot{e}_i(s) ds, \quad (38)$$

calculating the derivatives of $V(t)$ along the solutions of system (33), one has

$$\begin{aligned} \dot{V}(t) &= \sum_{i=1}^N e_i^T P \dot{e}_i(t) + \sum_{i=1}^N \left(\frac{T - \hat{\tau}_i(t)}{e^{2\xi t}} \right)' \int_{t-\hat{\tau}_i(t)}^t e^{2\xi s} \dot{e}_i^T(s) Q \dot{e}_i(s) \\ &\quad \cdot (s) ds + \sum_{i=1}^N (T - \hat{\tau}_i(t)) \left(\int_{t-\hat{\tau}_i(t)}^t e^{2\xi(s-t)} \dot{e}_i^T(s) Q \dot{e}_i(s) ds \right)' \end{aligned} \quad (39)$$

Noting that $\dot{\hat{\tau}}_i(t) = 1$ and $(de_i(t - \hat{\tau}_i(t))/dt) = \dot{e}_i(t - \hat{\tau}_i(t))(t - \hat{\tau}_i(t))' = 0$, then we have

$$\begin{aligned} \dot{V}(t) &= \sum_{i=1}^N e_i^T P \dot{e}_i(t) - 2\xi \sum_{i=1}^N (T - \hat{\tau}_i(t)) \int_{t-\hat{\tau}_i(t)}^t e^{2\xi(s-t)} \dot{e}_i^T(s) Q \dot{e}_i(s) \\ &\quad \cdot (s) ds - \sum_{i=1}^N \int_{t-\hat{\tau}_i(t)}^t e^{2\xi(s-t)} \dot{e}_i^T(s) Q \dot{e}_i(s) ds + \sum_{i=1}^N (T - \hat{\tau}_i \\ &\quad \cdot (t)) \dot{e}_i^T(s) Q \dot{e}_i(s) \\ &\leq \sum_{i=1}^N e_i^T P \dot{e}_i(t) - 2\xi \sum_{i=1}^N (T - \hat{\tau}_i(t)) \int_{t-\hat{\tau}_i(t)}^t e^{2\xi(s-t)} \dot{e}_i^T(s) Q \dot{e}_i(s) \\ &\quad \cdot (s) ds - e^{-2\xi T} \sum_{i=1}^N \int_{t-\hat{\tau}_i(t)}^t \dot{e}_i^T(s) Q \dot{e}_i(s) ds + \sum_{i=1}^N \\ &\quad \cdot (T - \hat{\tau}_i(t)) \dot{e}_i^T(s) Q \dot{e}_i(s). \end{aligned} \quad (40)$$

Thus, by using Kronecker product, we have

$$\begin{aligned} \dot{V}(t) + 2\xi V(t) &\leq e^T(t)(I_N \otimes P)\dot{e}(t) + \dot{e}^T(t)((TI_N - \hat{\tau}(t)) \otimes Q)\dot{e} \\ &\quad \cdot (t) - e^{-2\xi T} \sum_{i=1}^N \int_{t-\hat{\tau}_i(t)}^t \dot{e}_i^T(s) Q \dot{e}_i(s) ds \\ &\quad + 2\xi e^T(t)(I_N \otimes P)e(t). \end{aligned} \quad (41)$$

Let $\omega_i(t) = (1/\hat{\tau}_i(t)) \int_{t-\hat{\tau}_i(t)}^t \dot{e}_i(s) ds$; according to Jensen's inequality, one has

$$\int_{t-\hat{\tau}_i(t)}^t \dot{e}_i^T(s) Q \dot{e}_i(s) ds \geq \hat{\tau}_i(t) \omega_i^T(t) Q \omega_i(t). \quad (42)$$

Thus,

$$\begin{aligned} -e^{-2\xi T} \sum_{i=1}^N \int_{t-\hat{\tau}_i(t)}^t \dot{e}_i^T(s) Q \dot{e}_i(s) ds &\leq -e^{-2\xi T} \sum_{i=1}^N \hat{\tau}_i(t) \omega_i^T(t) Q \omega_i \\ &\quad \cdot (t) = -e^{-2\xi T} \omega^T(t) \\ &\quad \cdot (\hat{\tau}(t) \otimes Q) \omega(t), \end{aligned} \quad (43)$$

where $\omega^T(t) = [\omega_1^T(t), \omega_2^T(t), \dots, \omega_N^T(t)]$. From (33), the following equality can be derived:

$$\begin{aligned} 0 &= \sum_{i=1}^N 2[e_i^T(t)R + \dot{e}_i^T(t)S][\tilde{f}(t, e_i(t), e_i(t - \tau_1(t))) \\ &\quad + c_1 \sum_{j=1}^N a_{ij} \Gamma_1 e_j(t) + c_2 \sum_{j=1}^N b_{ij} \Gamma_2 e_j(t - \tau_2(t)) - d_i(e_i \\ &\quad \cdot (t - \hat{\tau}_i(t)) + \delta_i^s(t - \hat{\tau}_i(t))) - \dot{e}_i(t)]. \end{aligned} \quad (44)$$

By using Kronecker product again, we have

$$\begin{aligned}
0 = & 2e^T(t)(I_N \otimes R)\tilde{F} + 2c_1 e^T(t)(A \otimes R\Gamma_1)e(t) + 2c_2 e^T(t)(B \otimes R\Gamma_2)e(t - \tau_2(t)) \\
& - 2e^T(t)(D \otimes R)\delta^s(t - \hat{\tau}(t)) - 2e^T(t)(D \otimes R)e(t - \hat{\tau}(t)) - 2e^T(t)(I_N \otimes R)\dot{e}(t) \\
& + 2\dot{e}^T(t)(I_N \otimes S)\tilde{F} + 2c_1 \dot{e}^T(t)(A \otimes S\Gamma_1)e(t) + 2c_2 \dot{e}^T(t)(B \otimes S\Gamma_2)e(t - \tau_2(t)) \\
& - 2\dot{e}^T(t)(D \otimes S)\delta^s(t - \hat{\tau}(t)) - 2\dot{e}^T(t)(D \otimes S)e(t - \hat{\tau}(t)) - 2\dot{e}^T(t)(I_N \otimes S)\dot{e}(t).
\end{aligned} \tag{45}$$

Among the aforementioned equation, note that

$$-2e^T(t)(D \otimes R)\delta^s(t - \hat{\tau}(t)) \leq e^T(t)(D \otimes R)(D \otimes R)^T e(t) + \|\delta^s(t - \hat{\tau}(t))\|^2, \tag{46}$$

$$-2\dot{e}^T(t)(D \otimes S)\delta^s(t - \hat{\tau}(t)) \leq \dot{e}^T(t)(D \otimes R)(D \otimes S)^T \dot{e}(t) + \|\delta^s(t - \hat{\tau}(t))\|^2. \tag{47}$$

We can find from (41), (43), and (45)–(47) that

$$\begin{aligned}
\dot{V}(t) + 2\xi V(t) \leq & e^T(t)(I_N \otimes P)\dot{e}(t) + \dot{e}^T(t)((TI_N - \hat{\tau}(t)) \otimes Q)\dot{e}(t) + 2\xi e^T(I_N \otimes P)(t)e(t) \\
& - e^{-2\xi T} \omega^T(t)(\hat{\tau}(t) \otimes Q)\omega(t) + 2e^T(t)(I_N \otimes R)\tilde{F} + 2c_1 e^T(t)(A \otimes R\Gamma_1)e(t) \\
& + 2c_2 e^T(t)(B \otimes R\Gamma_2)e(t - \tau_2(t)) - 2e^T(t)(D \otimes R)e(t - \hat{\tau}(t)) \\
& - 2e^T(t)(I_N \otimes R)\dot{e}(t) - 2\dot{e}^T(t)(D \otimes S)e(t - \hat{\tau}(t)) - 2\dot{e}^T(t)(I_N \otimes S)\dot{e}(t) \\
& + 2\dot{e}^T(t)(I_N \otimes S)\tilde{F} + 2c_1 \dot{e}^T(t)(A \otimes S\Gamma_1)e(t) + 2c_2 \dot{e}^T(t)(B \otimes S\Gamma_2)e(t - \tau_2(t)) \\
& + e^T(t)(D \otimes R)(D \otimes R)^T e(t) + \dot{e}^T(t)(D \otimes R)(D \otimes S)^T \dot{e}(t) + 2\|\delta^s(t - \hat{\tau}(t))\|^2.
\end{aligned} \tag{48}$$

Then, one has

$$\dot{V}(t) + 2\xi V(t) \leq \eta^T(t)\Xi\eta(t) + 2\|\delta^s(t - \hat{\tau}(t))\|^2, \tag{49}$$

where $\eta(t) = [e^T(t), e^T(t - \tau_2(t)), e^T(t - \hat{\tau}(t)), \tilde{F}, \dot{e}^T(t), \omega^T(t)]$.

$$\Xi = \begin{pmatrix} \Xi_{11} & \Xi_{12} & \Xi_{13} & \Xi_{14} & \Xi_{15} & 0 \\ * & 0 & 0 & 0 & \Xi_{25} & 0 \\ * & * & 0 & 0 & \Xi_{35} & 0 \\ * & * & * & 0 & \Xi_{45} & 0 \\ * & * & * & * & \Xi_{55} & 0 \\ * & * & * & * & * & \Xi_{66} \end{pmatrix}, \tag{50}$$

where $\Xi_{55} = (TI_N - \hat{\tau}(t)) \otimes Q - 2(I_N \otimes S) + (DD^T \otimes SS^T)$, $\Xi_{66} = e^{-2\xi T}(\hat{\tau}(t) \otimes Q)$, and Ξ_{ij} has been given in Theorem 3. Let $\eta_0(t) = [e^T(t), e^T(t - \tau_2(t)), e^T(t - \hat{\tau}(t)), \tilde{F}, \dot{e}^T(t)]$, and based on the definition of Ξ_0 and Ξ_T , we have

$$\frac{TI_N - \hat{\tau}(t)}{T} \eta_0^T(t) \Xi_0 \eta_0(t) + \frac{\hat{\tau}(t)}{T} \eta^T(t) \Xi_T \eta(t) = \eta^T(t) \Xi \eta(t). \tag{51}$$

Thus, (35) and (36) imply that $\Xi < 0$; based on the definition of event-triggered instants, we have

$$\dot{V}(t) \leq -2\xi V(t) + N\alpha e^{-\beta t} + N\theta_0. \tag{52}$$

According to Lemma 2, we have

$$V(t) \leq \frac{N\theta_0}{2\xi} + \Psi e^{-2\xi(t-t_0)}, \tag{53}$$

where $\Psi = \sup_{-T \leq s \leq t_0} V(s)$. This completes our proof. \square

Remark 3. Note that the event-triggered instants t_k^i will be updated in some sampled instants; thus, it is easy to see the Zeno behavior will be excluded. Meanwhile, there were some published results which had investigated the synchronization problem about complex dynamical networks under the sampled control [23–25]. Compared with those results, the event-triggered strategy can reduce transmission frequency.

Remark 4. Some conditions formed as LMI have been obtained to guarantee the quasi-synchronization of CDNs under event-triggered with sampled data in Theorem 3. In which, the conditions can be checked by LMI toolbox of Matlab software directly and easily. However, the sampled period T needs to be given in the conditions; otherwise, the conditions cannot be regarded as LMI. It is obviously that the sampled-data period T cannot be chosen arbitrarily. Thus, it would be a significant problem that how to determine the maximum and minimum of sampled period T . This will be our future work.

Remark 5. This paper has investigated a CDN model with time-varying delays. However, it is not evident that how the time delays effect the synchronization behavior. Indeed, in the case of continuous data, we have used the generalized Halanay's inequality; this powerful tool just requires time delays to be bounded and the time delays can effect the rate of convergence μ^* . In the case of sampled data, to deal with the time delay, we have applied the well-known free-weighting matrix method, and one can see (41) and (43) in the proof of Theorem 3, then, the time delay has not appeared on the conditions. However, the conditions formed as LMIs in Theorem 3 are conservative. It is an interesting problem to analyse how can the time delays affect the synchronization in the sampled-data case and how to reduce the conservatism of the conditions in Theorem 3. They would be our future works.

4. Numerical Simulations

In this section, some examples will be given to check our theoretical result. An isolated dynamic behavior is described by a chaotic-delayed neural network at first. Then, quasi-synchronization for a coupled network under event-triggered controllers will be displayed. Finally, complete synchronization of the network under event-triggered controllers will be shown. Both continuous and sampled-data methods have been considered in the following examples. All the simulation results are based on the well-known fourth order Runge–Kutta method. The step in the simulation is set as 0.01. As for the sampled data, we used the

input-delay method in the simulation, which means that $\tau(t) = t - t_k$, then $t_k = t - \tau(t)$; consequently, the sampled-data system becomes to a time-delayed system, which also could be simulated by the Runge–Kutta method.

4.1. The Isolated Dynamic Behaviors. Suppose that the isolated dynamic behaviors can be described by the following delayed neural network:

$$\begin{aligned} \dot{s}(t) = f(t, s(t), s(t - \tau_1(t))) = Cs(t) + B_1 g_1(s(t)) + B_2 g_1 \\ \cdot (s(t - \tau_1(t))), \end{aligned} \quad (54)$$

where $s(t) = (s_1(t), s_2(t))^T \in \mathbb{R}^2$, $g_1(s(t)) = g_2(s(t)) = (\tanh(s_1(t)), \tanh(s_2(t)))^T$, $\tau_1 = 1$, and

$$\begin{aligned} C &= \begin{pmatrix} -1 & 0 \\ 0 & -1 \end{pmatrix}, \\ B_1 &= \begin{pmatrix} 2 & -0.1 \\ -5 & 4.5 \end{pmatrix}, \\ B_2 &= \begin{pmatrix} -1.5 & -0.1 \\ -0.2 & -4 \end{pmatrix}. \end{aligned} \quad (55)$$

The delayed neural network's state has a chaotic attractor as shown in Figure 1 with initial condition $\phi^s(t) = [0.1, 0.1]^T$ for $t \in [-1, 0]$.

Let us prove $f(t, x(t), x(t - \tau_1(t)))$ conforms with Assumption 1. In fact, for any $x(t) \in \mathbb{R}^n$, $y(t) \in \mathbb{R}^n$,

$$\begin{aligned} & (x(t) - y(t))^T (f(t, x(t), x(t - \tau_1(t))) - f(t, y(t), y(t - \tau_1(t)))) \\ &= (x(t) - y(t))^T (C(x(t) - y(t)) + B_1(g_1(x(t)) - g_1(y(t))) + B_2(g_2(x(t - \tau_1)) - g_2(y(t - \tau_1)))) \\ &= (x(t) - y(t))^T \left(\frac{C + C^T}{2} \right) (x(t) - y(t)) + (x(t) - y(t))^T B_1 (g_1(x(t)) - g_1(y(t))) + (x(t) - y(t))^T B_2 (g_2(x(t - \tau_1)) \\ & \quad - g_2(y(t - \tau_1))) \\ &\leq \lambda_{\max} \left(\frac{C + C^T}{2} + \left(\|B_1\| + \frac{\epsilon \|B_2\|}{2} \right) I_2 \right) (x(t) - y(t))^T (x(t) - y(t)) + \frac{\|B_1\|}{2} (g_1(x(t)) - g_1(y(t)))^T (g_1(x(t)) - g_1(y(t))) \\ & \quad + \frac{\|B_2\|}{2\epsilon} (g_2(x(t - \tau_1)) - g_2(y(t - \tau_1)))^T (g_2(x(t)) - g_2(y(t))) \\ &\leq \lambda_{\max} \left(\frac{C + C^T}{2} + \left(\|B_1\| + \frac{\epsilon \|B_2\|}{2} \right) I_2 \right) (x(t) - y(t))^T (x(t) - y(t)) + \frac{\|B_2\|}{2\epsilon} (x(t - \tau_1) - y(t - \tau_1))^T (x(t - \tau_1) - y(t - \tau_1)). \end{aligned} \quad (56)$$

Let $\epsilon = 5$, $L_1 = \lambda_{\max}(((C + C^T)/2) + (\|B_1\| + (\epsilon \|B_2\|/2)) I_2) = 15.9335$, and $L_2 = (\|B_2\|/2\epsilon) = 0.4009$; then, Assumption 1 can be guaranteed. Time delay can affect the dynamics of the node, and Figure 2 shows the different behaviors with different time delays.

4.2. Quasi-Synchronization for a Coupled Network under Event-Triggered Controllers. Consider the information interactive network with a communication graph given in Figure 3, and the corresponding adjacent matrix G is given by

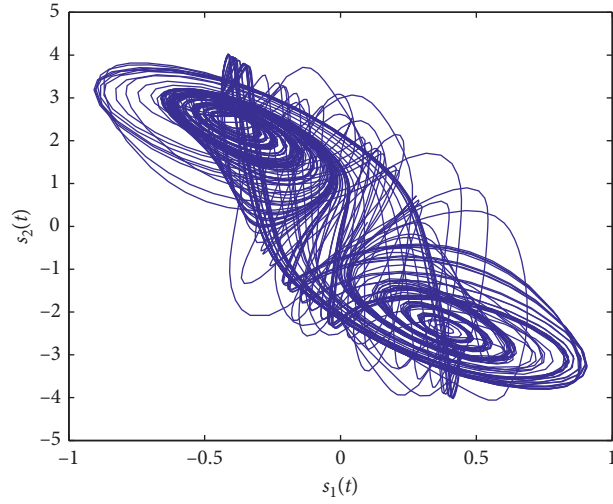


FIGURE 1: Chaotic attractor of $s(t)$.

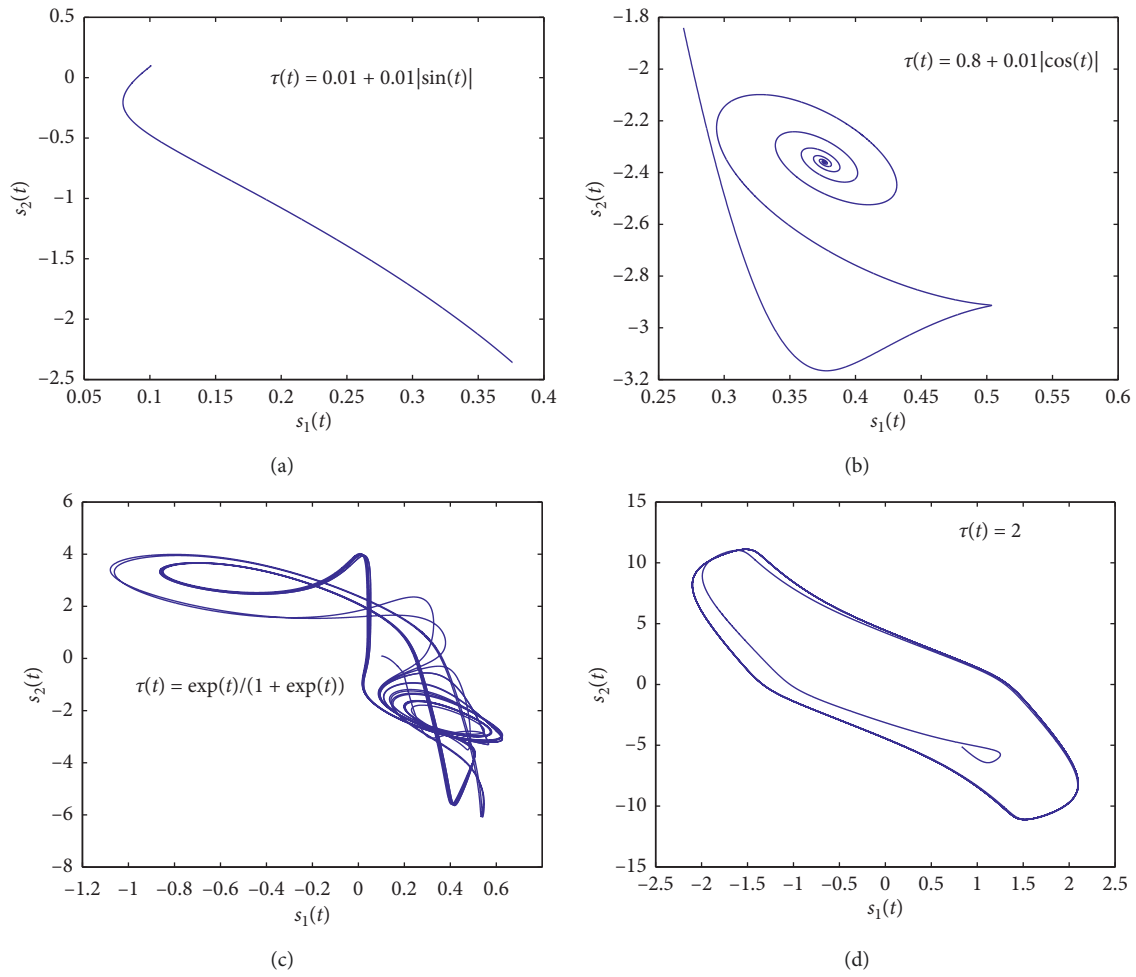


FIGURE 2: Different behaviors of $s(t)$ with different time delays.

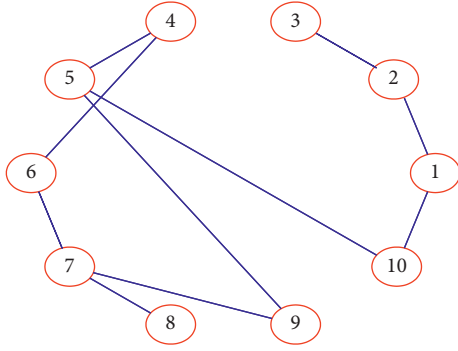


FIGURE 3: Interaction graph of 10 nodes.

$$G = \begin{pmatrix} 0 & 1 & 0 & 0 & 0 & 0 & 0 & 0 & 0 & 1 \\ 1 & 0 & 1 & 0 & 0 & 0 & 0 & 0 & 0 & 0 \\ 0 & 1 & 0 & 0 & 0 & 0 & 0 & 0 & 0 & 0 \\ 0 & 0 & 0 & 0 & 1 & 1 & 0 & 0 & 0 & 0 \\ 0 & 0 & 0 & 1 & 0 & 0 & 0 & 0 & 1 & 1 \\ 0 & 0 & 0 & 1 & 0 & 0 & 1 & 0 & 0 & 0 \\ 0 & 0 & 0 & 0 & 0 & 1 & 0 & 1 & 1 & 0 \\ 0 & 0 & 0 & 0 & 0 & 0 & 1 & 0 & 0 & 0 \\ 0 & 0 & 0 & 0 & 1 & 0 & 1 & 0 & 0 & 0 \\ 1 & 0 & 0 & 0 & 1 & 0 & 0 & 0 & 0 & 0 \end{pmatrix}, \quad (57)$$

where the weight configuration matrices A and B are $A = 15G$ and $B = 0.01G$, respectively. We also defined the inner coupling matrix $\Gamma_1 = 0.02\Gamma$ and $\Gamma_2 = 0.05\Gamma$, where

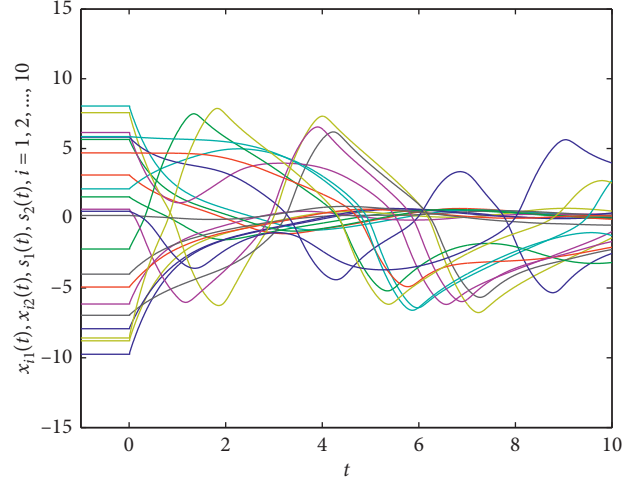
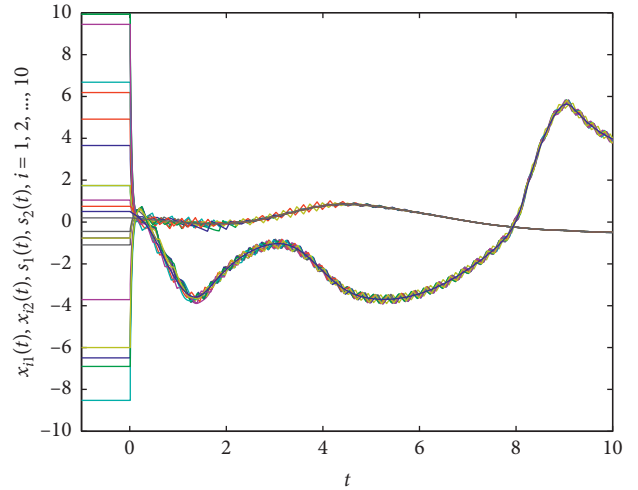
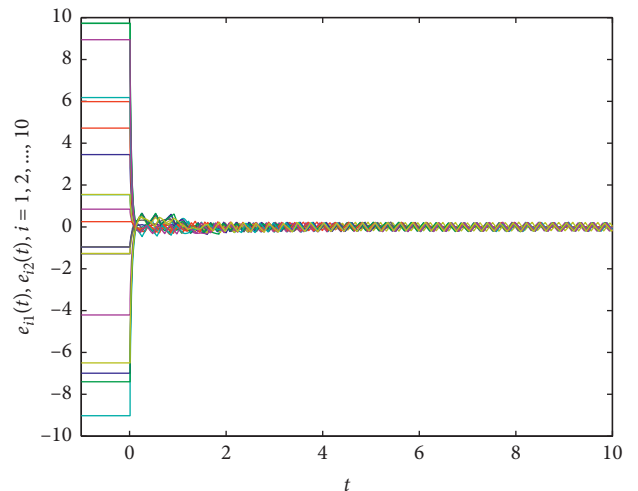
$$\Gamma = \begin{pmatrix} 0.2 & 0 \\ 0 & 0.2 \end{pmatrix}. \quad (58)$$

A constant coupled-delay $\tau_2 = 0.1$ has been considered in this example, and $c_1 = 1.8$, $c_2 = 1$. Without the control, the network cannot be synchronized to $s(t)$ by itself, and the state of its nodes and $s(t)$ can be seen in Figure 3.

Now, let us consider the event-triggered control. Let $\theta_0 = 0.5$, $\alpha = 0.1$, $\beta = 0.5$, and $\varepsilon = e$ for the threshold function $\theta(t)$. Also, given $D = 20I_{20}$. The following two examples are shown quasi-synchronized for a coupled network under event-triggered controllers with continuous feedback and sampled-data feedback, respectively (Figure 4).

From above parameters, one can calculate $\lambda_{\max}((2c_1\lambda_{\max}(A \otimes \Gamma_1) + c_2\omega_1\lambda_{\max}((BB^T) \otimes (\Gamma_2\Gamma_2^T)) + L_1 + p) - (2 - \omega_2)D) = -0.8687 < 0$ with $\omega_1 = \omega_2 = 1$, $p = 2$. Let $q = 1.4$, then, all conditions in Theorem 1 can be satisfied. Noting that, under these parameters, the quasi-synchronization can be derived, the errors are bounded. The synchronized states and synchronization errors are shown in Figures 5 and 6, respectively. Figure 7 shows the events of each node in time interval $[0, 1]$. The evolution of measurement errors under the event-triggered methods has been displayed in Figure 8.

Let sampled data period $T = 0.09$; based on LMI toolbox of Matlab, there exists P, Q, R , and S can satisfy conditions in

FIGURE 4: Time evolution of nodes' states $x_{i1}(t)$, $x_{i2}(t)$, and $s(t)$ without the control, $i = 1, 2, \dots, 10$.FIGURE 5: Time evolution of nodes' states $x_{i1}(t)$, $x_{i2}(t)$, and $s(t)$ with $\theta_0 = 0.5$ under continuous feedback, $i = 1, 2, \dots, 10$.FIGURE 6: Time evolution of synchronization errors $e_{i1}(t)$, $e_{i2}(t)$ with $\theta_0 = 0.5$ under continuous feedback, $i = 1, 2, \dots, 10$.

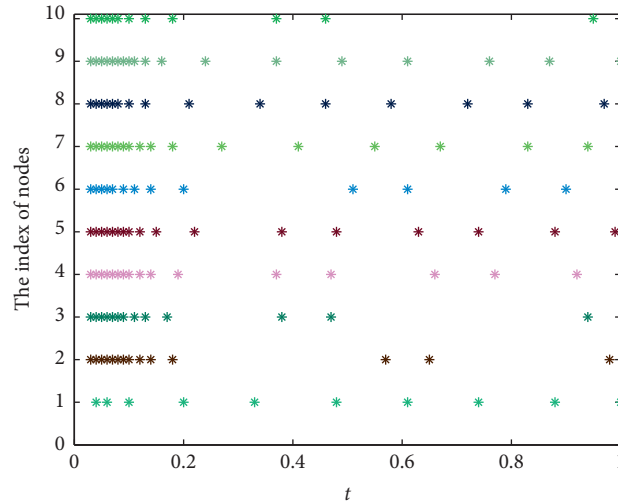


FIGURE 7: The events of each node with $\theta_0 = 0.5$ under continuous feedback, $i = 1, 2, \dots, 10$.

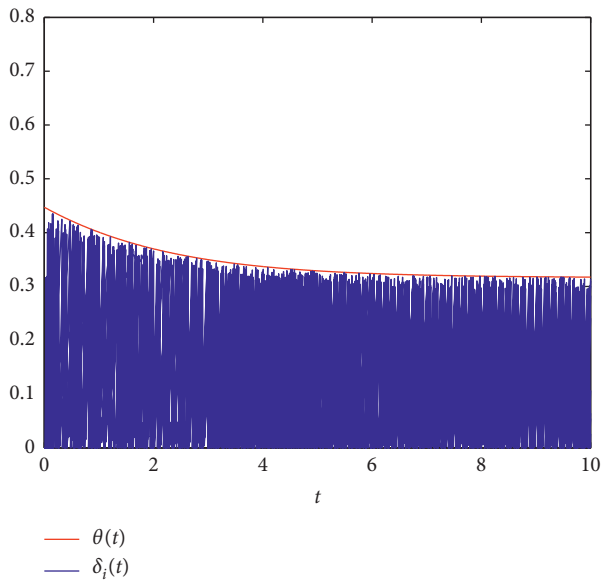


FIGURE 8: Evolution of measurement error and threshold with $\theta_0 = 0.5$ under continuous feedback, $i = 1, 2, \dots, 10$.

Theorem 2. Then, quasi-synchronization can be derived, and the errors are bounded. The synchronized states and synchronization errors are shown in Figures 9 and 10, respectively. Figure 11 shows the events of each node in time interval $[5, 10]$. The evolution of measurement errors under the event-triggered methods has been displayed in Figure 12.

In the following, we will compare the event-triggered method that has been used in this paper with some existed results. We will consider three cases: the sampled-data control method, event-triggered method with constant event threshold and based on sampled data, and event-triggered method with exponentially decreasing event threshold function and based on sampled data. The number of triggers with corresponding parameters has been listed in Table 1, in which we set the maximum of time as 10, and other parameters which are not mentioned in the table are the same

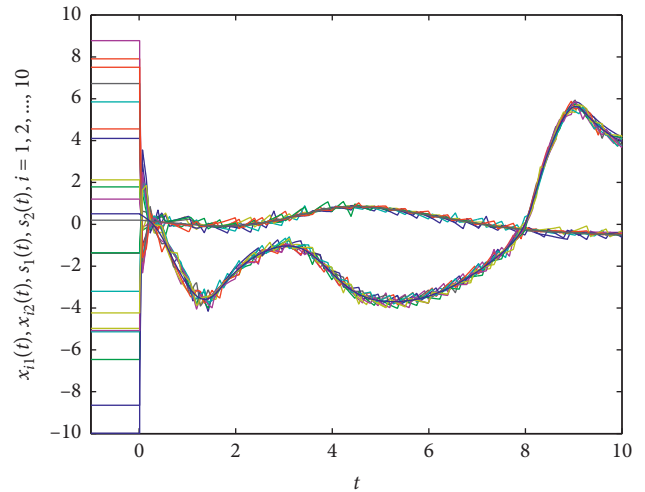


FIGURE 9: Time evolution of nodes' states $x_{i1}(t)$, $x_{i2}(t)$, and $s(t)$ with $\theta_0 = 0.5$ under sampled-data feedback, $i = 1, 2, \dots, 10$.

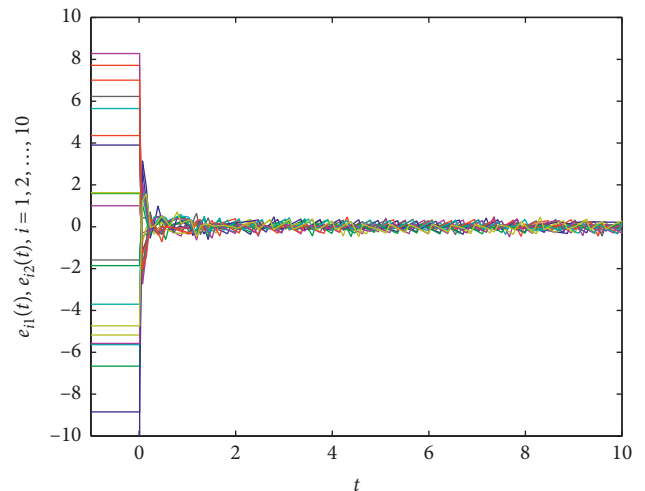


FIGURE 10: Time evolution of synchronization errors $e_{i1}(t)$, $e_{i2}(t)$ with $\theta_0 = 0.5$ under sampled-data feedback, $i = 1, 2, \dots, 10$.

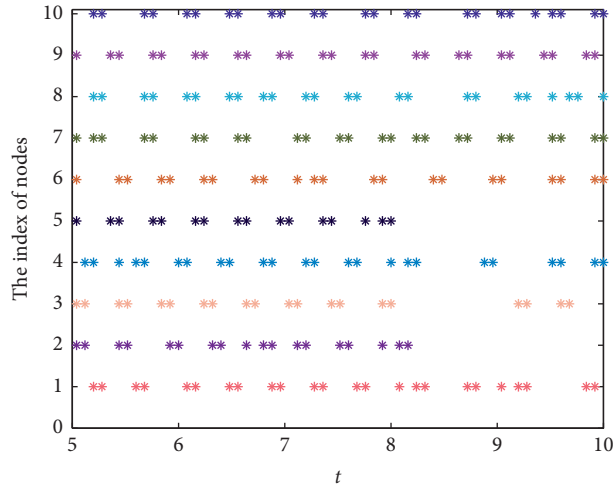


FIGURE 11: The events of each node with $\theta_0 = 0.5$ under sampled-data feedback, $i = 1, 2, \dots, 10$.

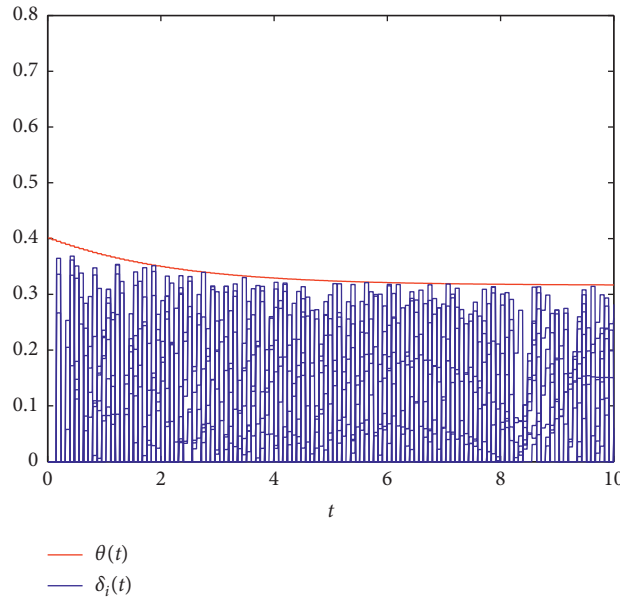


FIGURE 12: Evolution of measurement error and threshold with $\theta_0 = 0.5$ under sampled-data feedback, $i = 1, 2, \dots, 10$.

TABLE 1

T	θ_0	α	β	The number of trigger (sum of all nodes)
0.05	0	0	0	2000
0.05	0	1	0	1134
0.05	0	0.01	0	1277
0.05	0	0.5	0.5	1076

as above. The synchronization errors are shown in Figure 13, respectively.

Remark 6. According to above table, one has the number of trigger under the event-triggered method that has been used in this paper which is less than some other methods. It is obvious that less trigger times can provide a less update of information, which could reduce channel blockage. In

addition, from Figure 13, one can conclude that there is a better synchronization performance which can be obtained under our method.

4.3. Complete Synchronization of a Small-World Network under Event-Triggered Controllers. A small-world network with $N = 200$ nodes will be considered in this simulation. The small-world network is generated by taking initial

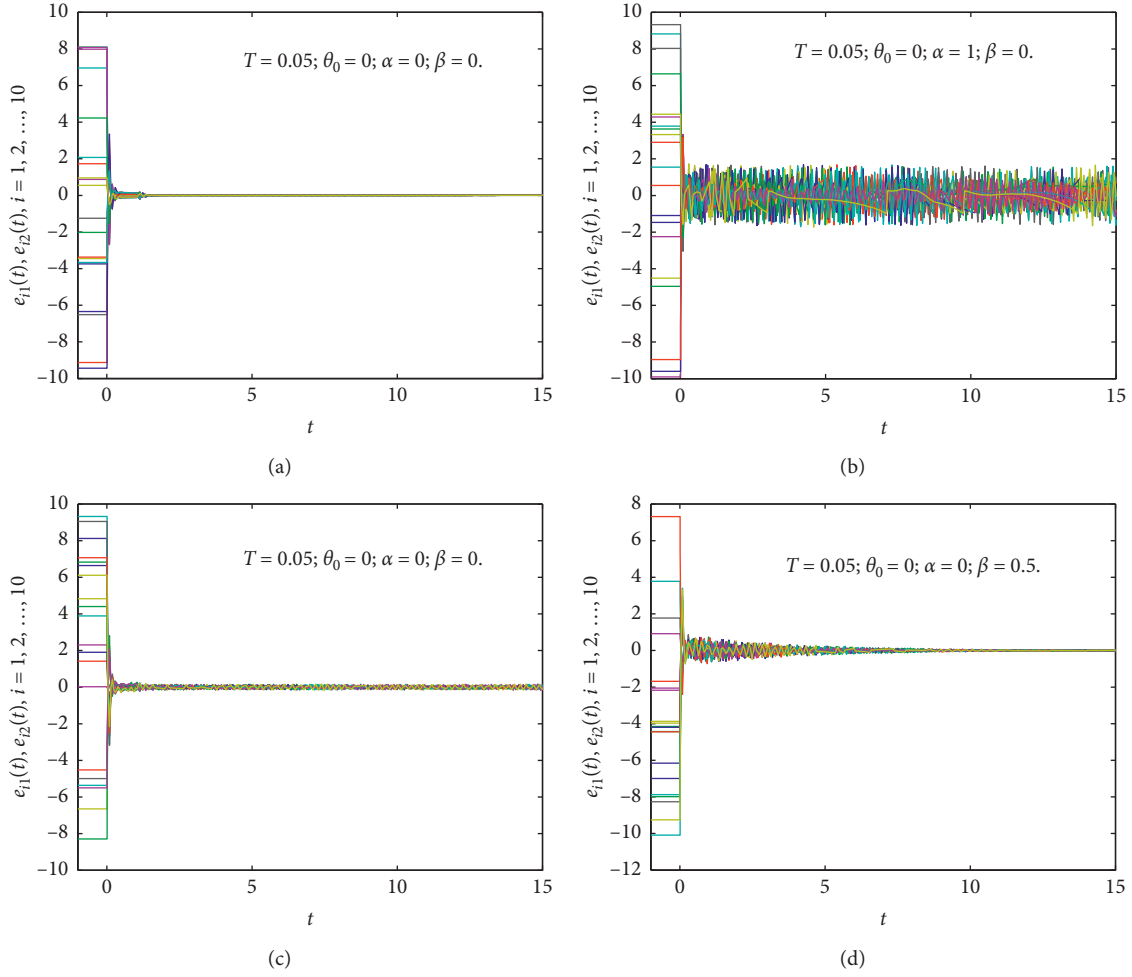


FIGURE 13: Time evolution of synchronization errors $e_{i1}(t)$, $e_{i2}(t)$ with different parameters in the above table, $i = 1, 2, \dots, 10$.

neighboring nodes $k = 8$ and the edge adding probability $p = 0.1$. Suppose that the adjacent matrix of the small-world network is G , which is defined as follows: if there is a connection between nodes i and j , then $g_{ij} = g_{ji} = 1$; otherwise $g_{ij} = g_{ji} = 0$. In this example, the weight configuration matrices A and B are $A = 15G$ and $B = 0.01G$, respectively. We also defined the inner coupling matrix $\Gamma_1 = 0.02\Gamma$ and $\Gamma_2 = 0.05\Gamma$, where

$$\Gamma = \begin{pmatrix} 0.01 & 0 \\ 0 & 0.02 \end{pmatrix}. \quad (59)$$

A constant coupled-delay $\tau_2 = 0.1$ has been considered in this example, and $c_1 = 1.8$, $c_2 = 1$. Without the control, the network cannot be synchronized to $s(t)$ by itself, and the state of its nodes and $s(t)$ can be seen in Figure 14.

Now, let us consider the event-triggered control. Let $\theta_0 = 0$, $\alpha = 0.1$, $\beta = 0.5$, and $\varepsilon = e$ for the threshold function $\theta(t)$. Also, given $D = 25I_{200}$. Then, one can calculate $\lambda_{\max}((2c_1\lambda_{\max}(A \otimes \Gamma_1) + c_2\omega_1\lambda_{\max}((BB^T) \otimes (\Gamma_2\Gamma_2^T)) + L_1 + p) - (2 - \omega_2)D) = -0.4 < 0$ with $\omega_1 = \omega_2 = 0$, $p = 2$. Let $q = 1.4$, then, all conditions in Theorem 1 can be satisfied. Noting that, under these parameters, the completed synchronization can be derived due to $\theta_0 = 0$. The synchronized states and

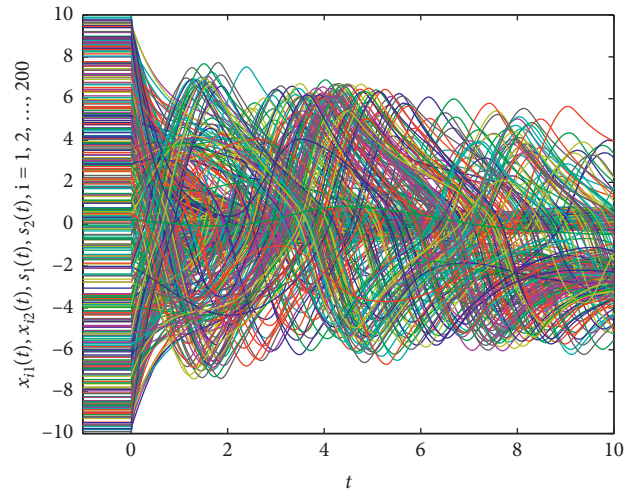


FIGURE 14: Time evolution of nodes' states $x_{i1}(t)$, $x_{i2}(t)$, and $s(t)$ without the control, $i = 1, 2, \dots, 200$.

synchronization errors under continuous feedback and sampled-data feedback with $T = 0.09$ are shown in Figures 15–18, respectively.

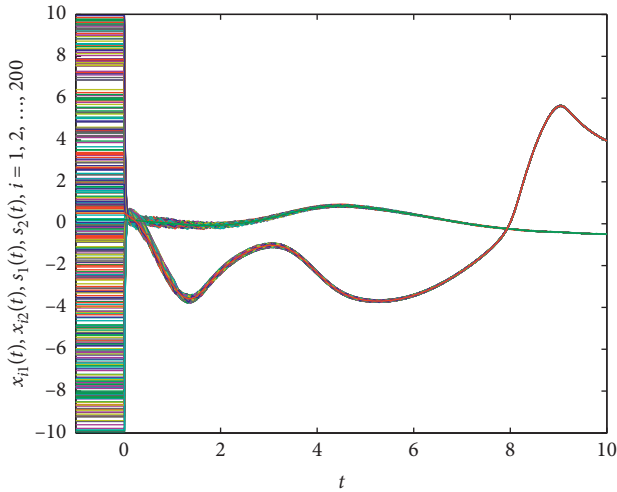


FIGURE 15: Time evolution of nodes' states $x_{i1}(t)$, $x_{i2}(t)$, and $s(t)$ under continuous feedback, $i = 1, 2, \dots, 200$.

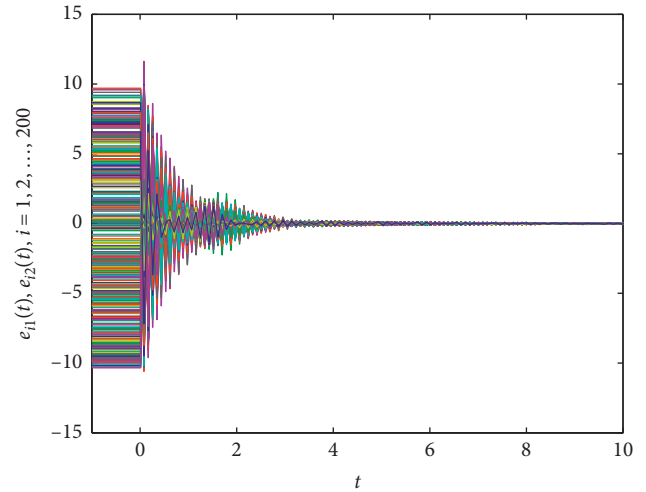


FIGURE 18: Time evolution of synchronization errors $e_{i1}(t)$, $e_{i2}(t)$ under sampled-data feedback, $i = 1, 2, \dots, 200$.

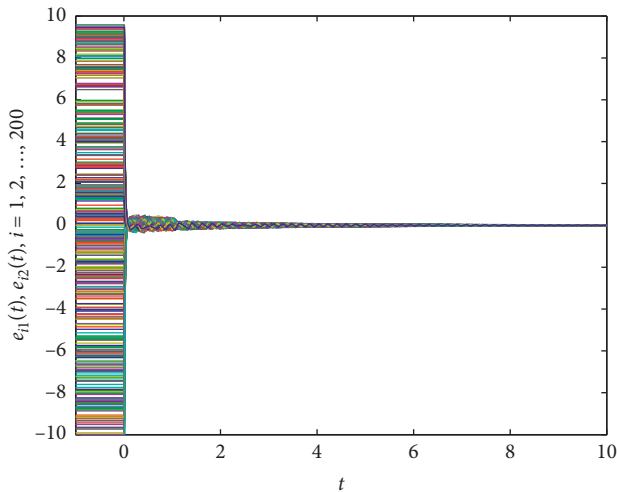


FIGURE 16: Time evolution of synchronization errors $e_{i1}(t)$, $e_{i2}(t)$ under continuous feedback, $i = 1, 2, \dots, 200$.

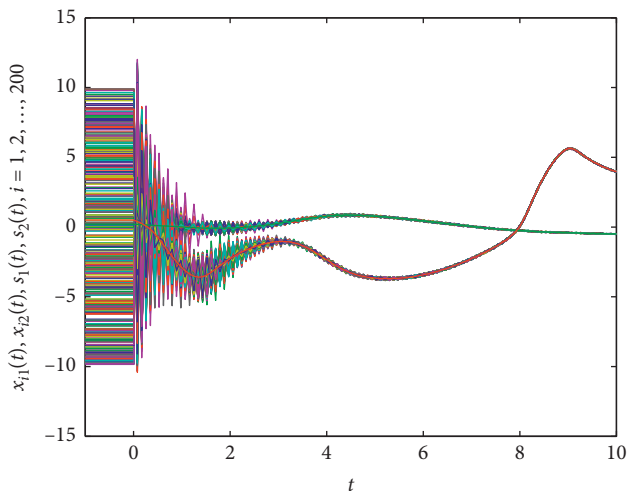


FIGURE 17: Time evolution of nodes' states $x_{i1}(t)$, $x_{i2}(t)$, and $s(t)$ under sampled-data feedback, $i = 1, 2, \dots, 200$.

5. Conclusion

In this paper, the event-triggered synchronization problem of the complex dynamical network has been studied. Both continuous feedback and sampled-data feedback control methods have been studied. In the case of continuous feedback control approach, the Zeno behavior has been excluded. The main theoretical results are derived based on Lyapunov stability and generalized Halanay's inequality. In addition, both internal delay and coupling delay have been considered in the complex dynamical model. The given numerical examples illustrate the corresponding theoretical analysis. Extending the proposed approach to the consensus of multiagent systems will be our future works. In addition, in the sampled-data case, this paper just has considered the periodic situation. However, it would be more challenging and interesting to study the event-triggered method based on aperiodic sampled data. Some external disturbances also could be taken into account, such as impulsive and stochastic noise. All of them will be our future works.

Data Availability

All data are shown in the simulation part of the manuscript.

Conflicts of Interest

The authors declare that they have no conflicts of interest.

Acknowledgments

This work was jointly supported by the Natural Science Foundation of Shandong Province of China under Grant no. ZR2019MA034 and the Natural Science Foundation of Jiangsu Province of China under Grant no. BK20161126.

References

- [1] S. H. Strogatz, "Exploring complex networks," *Nature*, vol. 410, no. 6825, pp. 268–276, 2001.
- [2] R. Albert and A.-L. Barabási, "Statistical mechanics of complex networks," *Reviews of Modern Physics*, vol. 74, no. 1, pp. 47–97, 2002.
- [3] J. Lü, X. Yu, and G. Chen, "Chaos synchronization of general complex dynamical networks," *Physica A: Statistical Mechanics and Its Applications*, vol. 334, no. 1-2, pp. 281–302, 2004.
- [4] X. F. Wang, "Complex networks: topology, dynamics and synchronization," *International Journal of Bifurcation and Chaos*, vol. 12, no. 5, pp. 885–916, 2002.
- [5] B. Mauricio and L. Pecora, "Synchronization in small-world systems," *Physical Review Letters*, vol. 89, no. 5, Article ID 054101, 2002.
- [6] A. Arenas, A. Díaz-Guilera, J. Kurths, Y. Moreno, and C. Zhou, "Synchronization in complex networks," *Physics Reports*, vol. 469, no. 3, pp. 93–153, 2008.
- [7] J. Wang, X. Hu, Y. Wei, and Z. Wang, "Sampled-data synchronization of semi-markov jump complex dynamical networks subject to generalized dissipativity property," *Applied Mathematics and Computation*, vol. 346, no. 4, pp. 853–864, 2019.
- [8] D. Zeng, R. Zhang, X. Liu, S. Zhong, and K. Shi, "Pinning stochastic sampled-data control for exponential synchronization of directed complex dynamical networks with sampled-data communications," *Applied Mathematics and Computation*, vol. 337, no. 11, pp. 102–118, 2018.
- [9] P. Selvaraj, R. Sakthivel, and C. Ahn, "Observer-based synchronization of complex dynamical networks under actuator saturation and probabilistic faults," *IEEE Transactions on Systems, Man, and Cybernetics: Systems*, vol. 49, no. 7, pp. 1516–1526, 2018.
- [10] H.-L. Li, J. Cao, H. Jiang, and A. Alsaedi, "Graph theory-based finite-time synchronization of fractional-order complex dynamical networks," *Journal of the Franklin Institute*, vol. 355, no. 13, pp. 5771–5789, 2018.
- [11] Y. Wu, Y. Li, and W. Li, "Synchronization of random coupling delayed complex networks with random and adaptive coupling strength," *Nonlinear Dynamics*, vol. 96, no. 4, pp. 2393–2412, 2019.
- [12] N. Li, X. Wu, J. Feng, and Y. Wu, "Fixed-time synchronization in probability of drive-response networks with discontinuous nodes and noise disturbances," *Nonlinear Dynamics*, vol. 97, no. 1, pp. 297–311, 2019.
- [13] F. Wang and Y. Yang, "Quasi-synchronization for fractional-order delayed dynamical networks with heterogeneous nodes," *Applied Mathematics and Computation*, vol. 339, pp. 1–14, 2018.
- [14] P. Selvaraj, O. M. Kwon, and R. Sakthivel, "Disturbance and uncertainty rejection performance for fractional-order complex dynamical networks," *Neural Networks*, vol. 112, pp. 73–84, 2019.
- [15] B. Yang, X. Wang, J. Fang, and Y. Xu, "The impact of coupling function on finite-time synchronization dynamics of multi-weighted complex networks with switching topology," *Complexity*, vol. 2019, Article ID 7276152, 15 pages, 2019.
- [16] Y. Luo, L. Shu, and B. Zhou, "Global exponential synchronization of nonlinearly coupled complex dynamical networks with time-varying coupling delays," *Complexity*, vol. 2017, Article ID 7850958, 10 pages, 2017.
- [17] L. Yan and J. Li, "Adaptive aperiodically intermittent synchronization for complex dynamical network with unknown time-varying outer coupling strengths," *Mathematical Problems in Engineering*, vol. 2019, Article ID 6732357, 12 pages, 2019.
- [18] J. Fang, N. Liu, and J. Sun, "Adaptive modified function projective synchronization of uncertain complex dynamical networks with multiple time-delay couplings and disturbances," *Mathematical Problems in Engineering*, vol. 2018, Article ID 6384757, 11 pages, 2018.
- [19] W. Zhang, J. Cao, D. Chen, and A. Alsaedi, "Out lag synchronization of fractional order delayed complex networks with coupling delay via pinning control," *Complexity*, vol. 2019, Article ID 5612150, 7 pages, 2019.
- [20] X. Wang, X. Liu, K. She, and S. Zhong, "Pinning impulsive synchronization of complex dynamical networks with various time-varying delay sizes," *Nonlinear Analysis: Hybrid Systems*, vol. 26, no. 11, pp. 307–318, 2017.
- [21] R. Rakkiyappan, G. Velmurugan, J. Nicholas George, and R. Selvamani, "Exponential synchronization of Lur'e complex dynamical networks with uncertain inner coupling and pinning impulsive control," *Applied Mathematics and Computation*, vol. 307, no. 8, pp. 217–231, 2017.
- [22] P. Selvaraj, R. Sakthivel, and O. M. Kwon, "Synchronization of fractional-order complex dynamical network with random coupling delay, actuator faults and saturation," *Nonlinear Dynamics*, vol. 94, no. 4, pp. 3101–3116, 2018.
- [23] N. Li, Y. Zhang, J. Hu, and Z. Nie, "Synchronization for general complex dynamical networks with sampled-data," *Neurocomputing*, vol. 74, no. 5, pp. 805–811, 2011.
- [24] R. Rakkiyappan, N. Sakthivel, and J. Cao, "Stochastic sampled-data control for synchronization of complex dynamical networks with control packet loss and additive time-varying delays," *Neural Networks*, vol. 66, no. 6, pp. 46–63, 2015.
- [25] Z. Chen, K. Shi, and S. Zhong, "New synchronization criteria for complex delayed dynamical networks with sampled-data feedback control," *ISA Transactions*, vol. 63, no. 7, pp. 154–169, 2016.
- [26] D. Zeng, R. Zhang, Y. Liu, and S. Zhong, "Sampled-data synchronization of chaotic Lur'e systems via input-delay-dependent-free-matrix zero equality approach," *Applied Mathematics and Computation*, vol. 315, no. 12, pp. 34–46, 2017.
- [27] L. Wu, Y. Gao, J. Liu, and H. Li, "Event-triggered sliding mode control of stochastic systems via output feedback," *Automatica*, vol. 82, no. 8, pp. 79–92, 2017.
- [28] W. Xu, D. W. C. Ho, L. Li, and J. Cao, "Event-triggered schemes on leader-following consensus of general linear multiagent systems under different topologies," *IEEE Transactions on Cybernetics*, vol. 47, no. 1, pp. 212–223, 2017.
- [29] Q. Li, S. Liu, and Y. Chen, "Combination event-triggered adaptive networked synchronization communication for nonlinear uncertain fractional-order chaotic systems," *Applied Mathematics and Computation*, vol. 333, no. 9, pp. 521–535, 2018.
- [30] L. Zou, Z.-D. Wang, and D.-H. Zhou, "Event-based control and filtering of networked systems: a survey," *International Journal of Automation and Computing*, vol. 14, no. 3, pp. 239–253, 2017.
- [31] C. Peng and F. Li, "A survey on recent advances in event-triggered communication and control," *Information Sciences*, vol. 457–458, no. 8, pp. 113–125, 2018.

- [32] S. Lv, W. He, F. Qian, and J. Cao, "Leaderless synchronization of coupled neural networks with the event-triggered mechanism," *Neural Networks*, vol. 105, no. 9, pp. 316–327, 2018.
- [33] Y. Liu, B. Jiang, J. Lu, J. Cao, and G. Lu, "Event-triggered sliding mode control for attitude stabilization of a rigid spacecraft," *IEEE Transactions on Systems, Man, and Cybernetics: Systems*, pp. 1–10, 2018.
- [34] J. Zhou, H. Dong, and J. Feng, "Event-triggered communication for synchronization of markovian jump delayed complex networks with partially unknown transition rates," *Applied Mathematics and Computation*, vol. 293, pp. 617–629, 2017.
- [35] J. Yang, J. Lu, L. Li, Y. Liu, Z. Wang, and F. Alsaadi, "Event-triggered control for the synchronization of Boolean control networks," *Nonlinear Dynamics*, vol. 96, no. 2, pp. 1335–1344, 2019.
- [36] S. Zhu, J. Lou, Y. Liu, Y. Li, and Z. Wang, "Event-triggered control for the stabilization of probabilistic Boolean control networks," *Complexity*, vol. 2018, Article ID 9259348, 7 pages, 2018.
- [37] B. Li, Y. Liu, K. Kou, and L. Yu, "Event-triggered control for the disturbance decoupling problem of Boolean control networks," *IEEE Transactions on Cybernetics*, vol. 48, no. 9, pp. 2764–2769, 2017.
- [38] S. Wen, Z. Zeng, M. Z. Q. Chen, and T. Huang, "Synchronization of switched neural networks with communication delays via the event-triggered control," *IEEE Transactions on Neural Networks and Learning Systems*, vol. 28, no. 10, pp. 2334–2343, 2017.
- [39] Y. Liu, J. H. Park, B.-Z. Guo, F. Fang, and F. Zhou, "Event-triggered dissipative synchronization for Markovian jump neural networks with general transition probabilities," *International Journal of Robust and Nonlinear Control*, vol. 28, no. 13, pp. 3893–3908, 2018.
- [40] J. Lunze and D. Lehmann, "A state-feedback approach to event-based control," *Automatica*, vol. 46, no. 1, pp. 211–215, 2010.
- [41] J. Zhang and G. Feng, "Event-driven observer-based output feedback control for linear systems," *Automatica*, vol. 50, no. 7, pp. 1852–1859, 2014.
- [42] F. Wang and Y. Yang, "Leader-following consensus of nonlinear fractional-order multi-agent systems via event-triggered control," *International Journal of Systems Science*, vol. 48, no. 3, pp. 571–577, 2017.
- [43] F. Wang, Y. Yang, and X. Xu, "Synchronization of complex dynamical networks via sampled-data control: a threshold function event-triggered method," in *Proceedings of the 2017 29th Chinese Control and Decision Conference*, vol. 7, pp. 7515–7560, IEEE, Chongqing, China, May 2017.
- [44] B. Yang, X. Wang, Y. Zhang, Y. Xu, and W. Zhou, "Finite-time synchronization and synchronization dynamics analysis for two classes of Markovian switching multiweighted complex networks from synchronization control rule viewpoint," *Complexity*, vol. 2019, Article ID 1921632, 17 pages, 2019.
- [45] J. Chen and X. Chen, *Special Matrices*, Tsinghua University Press, Beijing, China, 2001.
- [46] L. Wen, Y. Yu, and W. Wang, "Generalized halanay inequalities for dissipativity of volterra functional differential equations," *Journal of Mathematical Analysis and Applications*, vol. 347, no. 1, pp. 169–178, 2008.



Hindawi

Submit your manuscripts at
www.hindawi.com

